Cancer Research

CSF1/CSF1R Blockade Reprograms Tumor-Infiltrating Macrophages and Improves Response to T-cell Checkpoint Immunotherapy in Pancreatic Cancer Models

Yu Zhu[1,2], Brett L. Knolhoff[1,2], Melissa A. Meyer[1,2], Timothy M. Nywening[3,4], Brian L. West[5], Jingqin Luo[4,6], Andrea Wang-Gillam[1], S. Peter Goedegebuure[3,4], David C. Linehan[3,4], and David G. DeNardo[1,2,4,7]

Abstract

Cancer immunotherapy generally offers limited clinical benefit without coordinated strategies to mitigate the immunosuppressive nature of the tumor microenvironment. Critical drivers of immune escape in the tumor microenvironment include tumor-associated macrophages and myeloid-derived suppressor cells, which not only mediate immune suppression, but also promote metastatic dissemination and impart resistance to cytotoxic therapies. Thus, strategies to ablate the effects of these myeloid cell populations may offer great therapeutic potential. In this report, we demonstrate in a mouse model of pancreatic ductal adenocarcinoma (PDAC) that inhibiting signaling by the myeloid growth factor receptor CSF1R can functionally reprogram macrophage responses that enhance antigen presentation and productive antitumor T-cell responses. Investigations of this response revealed that CSF1R blockade also upregulated T-cell checkpoint molecules, including PDL1 and CTLA4, thereby restraining beneficial therapeutic effects. We found that PD1 and CTLA4 antagonists showed limited efficacy as single agents to restrain PDAC growth, but that combining these agents with CSF1R blockade potently elicited tumor regressions, even in larger established tumors. Taken together, our findings provide a rationale to reprogram immunosuppressive myeloid cell populations in the tumor microenvironment under conditions that can significantly empower the therapeutic effects of checkpoint-based immunotherapeutics. *Cancer Res; 74(18); 5057–69. ©2014 AACR.*

Introduction

Pancreatic ductal adenocarcinoma (PDAC) is one of the most lethal human malignancies. Current therapies are ineffective at treating late stage disease. The few durable responses to therapy seen in patients with PDAC are often associated with significant cytotoxic lymphocyte (CTL) infiltration into tumor tissue, suggesting that effective immunotherapy would hold promise to improve patient outcome (1, 2). However, attempts to use immunotherapeutics as single agents have achieved only limited clinical success (3, 4). Although multiple factors can contribute to the resistance of PDAC to immunotherapies, one dominant player is the presence of a suppressive immune microenvironment. Critical drivers of this immunosuppressive microenvironment include tumor-associated macrophages (TAM), monocytic myeloid-derived suppressor cells (Mo-MDSC), and granulocytic MDSCs (G-MDSC). These leukocytes can also promote tumor cell proliferation, confer resistance to cytotoxic stress, and facilitate metastatic dissemination (5, 6). Therefore, high numbers of tumor-infiltrating myeloid cells often correlate with early local or metastatic relapse, leading to poor survival in patients with pancreatic cancer (7–9). Therapeutics that can reprogram these myeloid responses might overcome immunosuppression to enhance responses to immunotherapy. Previous work by our group and others demonstrated that combining cytotoxic chemotherapy with the blockade of colony-stimulating factor 1 receptor (CSF1R), which is prominently expressed by monocytes, Mo-MDSCs, and macrophages, results in improved antitumor T-cell responses (10–12). These data suggest that CSF1R blockade could be effective at alleviating local tumor-induced immune suppression and bolstering the response to immunotherapy.

In this report, we investigate the mechanisms by which inhibition of CSF1R signaling alleviates immune suppression. We demonstrate that CSF1/CSF1R blockade not only decreases the number of TAMs, but also reprograms remaining TAMs to support antigen presentation and bolster T-cell activation within the tumor microenvironment. This in-turn

[1]Department of Medicine, Washington University School of Medicine, St Louis, Missouri. [2]BRIGHT Institute, Washington University School of Medicine, St Louis, Missouri. [3]Department of Surgery, Washington University School of Medicine, St Louis, Missouri. [4]Siteman Cancer Center, Washington University School of Medicine, St Louis, Missouri. [5]Plexxikon Inc., Berkeley, California. [6]Division of Biostatistics, Washington University School of Medicine, St Louis, Missouri. [7]Department of Pathology and Immunology, Washington University School of Medicine, St Louis, Missouri.

Note: Supplementary data for this article are available at Cancer Research Online (http://cancerres.aacrjournals.org/).

Corresponding Author: David G. DeNardo, Department of Medicine, 660 South Euclid Avenue, Box 8069, St Louis, MO 63110. Phone: 314-362-9524; Fax: 314-747-2797; E-mail: ddenardo@dom.wustl.edu

doi: 10.1158/0008-5472.CAN-13-3723

leads to reduced immune suppression and elevated interferon responses, which restrain tumor progression. However, in response to reduced immune suppression, programmed death 1 ligand 1 (PDL1) is upregulated on tumor cells and cytotoxic T lymphocyte antigen 4 (CTLA4) on T cells. These checkpoint molecules limit the potential of CSF1R inhibition to stimulate antitumor immunity. Both programmed cell death protein 1 (PD1) and CTLA4 antagonists demonstrate limited ability to restrain PDAC growth in this mouse model, similar to reported efficacy as single agents in patients with PDAC (3, 4). However, CSF1R blockade overcomes these limitations to achieve regression in even well-established tumors. These data suggest that reprogramming myeloid cell responses via CSF1/CSF1R blockade could improve the efficacy of checkpoint-based immunotherapeutics.

Materials and Methods

Pancreatic cancer tissue microarray cohort and analysis

Tissue microarray (TMA) studies were conducted on surgically resected PDAC specimens from 60 patients diagnosed in the Department of Pathology at Washington University (St. Louis, MO). Patients underwent pancreaticoduodenectomy followed by adjuvant chemotherapy. Fifty-nine of the 60 patients did not receive neoadjuvant therapy. To assemble TMAs, clearly defined areas of tumor tissue were demarcated and two biopsies (1.0-mm diameter) were taken from each donor block. The Washington University School of Medicine ethics committee approved this study. Fully automated image acquisition was performed using an Aperio ScanScope XT Slide Scanner system with a ×20 objective (Aperio Technologies) to capture whole-slide digital images. Fluorescent staining analysis was performed using MetaMorph software.

IHC

Tissues were fixed in 10% formalin, embedded in paraffin, and dehydrated in 70% ethanol. Of note, 5-μm-thick sections were deparaffinized in xylene, rehydrated in graded ethanol, and subjected to antigen retrieval by steam heating in Citra antigen retrieval solution (BioGenex). CSF1 was stained with clone 2D10 at 1:100 (Thermo) and detected using indirect immunofluorescence.

Cell lines and constructs

KC cells were derived from PDAC tumor tissue obtained from p48-CRE/LSL-KRas/$p53^{flox/flox}$ mice (backcrossed C57/B6, $n = 6$ by speed congenic) by our laboratory. Kras-INK (KI) cells were obtained from Dr. Hanahan's laboratory (13, 14). All cell lines were negative for MAP and mycoplasma. Subsets of these cells were labeled with a polycistronic click beetle red luciferase-mCherry reporter.

Orthotopic model and preclinical animal cohorts

Syngeneic orthotopic PDAC tumors were established by surgical implantation, as previously described (15). Briefly, we injected 200,000 cells in 50 μL Matrigel (BD Biosciences) into each mouse's pancreas. Cohorts of mice were randomized into different treatment groups by either bioluminescence imaging on day 12 or gross palpation of the pancreas. Mice were treated with 50 mg/kg gemcitabine (GEM; Hospira) by intravenous (i.v.) injection into the right retro-orbital sinus every 4 to 5 days. Preclinical studies were conducted with 10 to 15 10-week-old female mice per group. Tumor burden was measured by establishing gross wet weight of the pancreas/tumor and comparing it with that of 5 parallel mice sacrificed at the beginning of treatment. All studies involving animals were approved by the Washington University School of Medicine Institutional Animal Studies Committee.

CSF1R inhibitors, CSF1 neutralizing antibodies, and checkpoint antagonists

CSF1 neutralizing antibody (clone 5A1, BioXCell) was administered via intraperitoneal (i.p.) injection every 4 to 5 days, with the first injection containing 1 mg and subsequent injections 0.5 mg. CSF1R inhibitors (CSF1Ri) were provided by Plexxikon Inc. PLX3397 is a selective bispecific inhibitor for c-Fms and the c-Kit receptor tyrosine kinases (12, 16–17). GW2580 has been described in detail previously (18). Both GW2580 and PLX3397 were administered at 800 mg/kg in chow. CTLA4 and PD1 antagonists (clones UC10-4F10 and RMP1-14, BioXCell) were given every 4 to 5 days at 250 and 200 μg/dose, respectively.

Flow-cytometric analysis

Single-cell suspensions were prepared from dissected pancreatic tumors by manual mincing using a scalpel, followed by enzymatic digestion with 3.0 mg/mL collagenase A (Roche) and DNase I (Sigma) for 30 minutes at 37°C with constant stirring. Digestion mixtures were quenched by 10% FBS, and filtered through 40-μm nylon strainers (Fisher Scientific). Cells were incubated for 10 minutes at 4°C with rat anti-mouse CD16/CD32 mAb (eBioscience) at 1:200 dilution. Cells were washed twice in PBS/BSA and incubated for 20 minutes with 100 μL of fluorophore-conjugated anti-mouse antibodies [CD3e (145-2C11), CD4 (GK1.5), CD8a (53-6.7), CD11b (M1/70), CD11c (N418), CD19 (MB19-1), Ly6C (HK1.4), CD45 (30-F11), CD115 (AFS98), F4/80 (BM8), MHCII (M5/114.15.2), FoxP3 (FJK-16s), CD44 (IM7), CD69 (H1.2F3), PD1 (J43), PDL1 (MIH5), PDL2 (122), CTLA4 (UC10-4B9), IgG2α/κ (eBR2a)], (all from eBioscience) and/or Ly6G (1A8, BioLegend), and CD206 (MR5D3, AbDSerotec) using the manufacturers' recommended concentrations. Data acquisition was performed on the LSR-II system (BD Biosciences) and FlowJo software version 9.2 (Tree Star) was used for analysis.

Additional details are in the Supplementary Data.

Results

CSF1 is overexpressed by human PDAC cells

Previously, we reported that inhibition of CSF1/CSF1R signaling could improve the efficacy of chemotherapy in murine PDAC models by enhancing chemotherapy-induced antitumor immunity (11). However, the mechanisms by which inhibition of CSF1/CSF1R signaling regulates antitumor immunity are not well understood. To determine the cellular sources of CSF1 and CSF1R in human pancreatic cancer

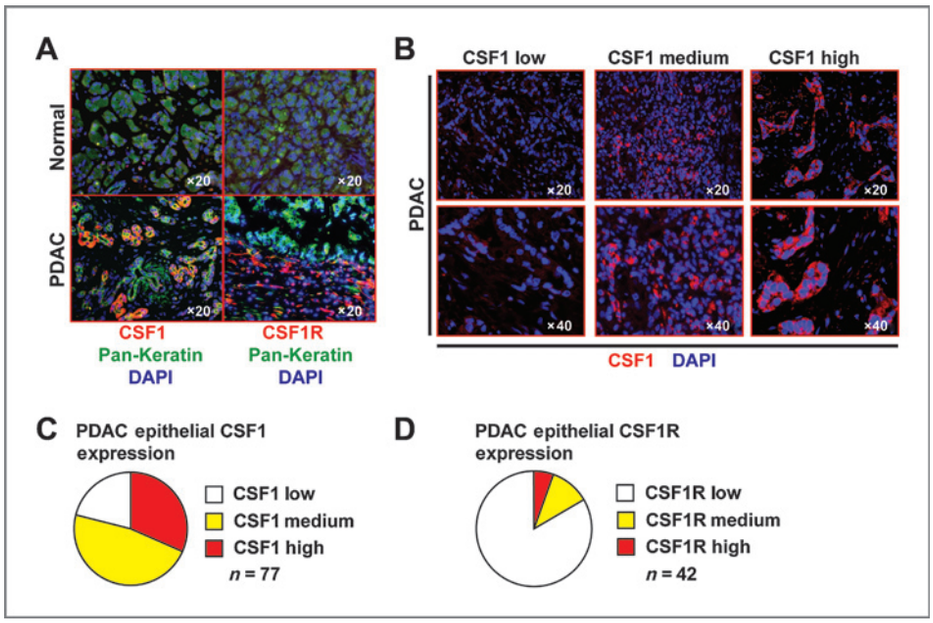

Figure 1. PDAC tumors overexpress CSF1. A–B, IHC analysis of CSF1 expression in normal pancreas and PDAC tissue. Representative immunofluorescent images are shown. C–D, stratification of patient PDAC samples based on expression levels of CSF1 and CSF1R ($n = 4$ normal and 77 PDAC).

patients, we analyzed TMAs constructed from 77 cases of invasive PDAC and four samples of normal pancreatic tissue. IHC staining showed that CSF1 is frequently, but not exclusively, expressed by malignant PDAC cells (Fig. 1A). In addition, tumors frequently had elevated expression of CSF1 compared with normal tissue. PDAC cells in 70% of tumor specimens exhibited moderate to high levels of CSF1 expression (Fig. 1A–C). In contrast, CSF1R was frequently detected in the tumor stroma, whereas only approximately 10% of the tumors examined had CSF1R expression in the epithelial compartment (Fig. 1A and D). These observations are consistent with other reports (19, 20) and suggest that PDAC tumor cells frequently produce high levels of CSF1.

Inhibition of CSF1R signaling reprograms the tumor microenvironment

To understand the impact of CSF1R signaling on the tumor microenvironment, we compared the gene expression profile of PDAC tumor tissue following treatment with either CSF1R inhibitors (CSF1Ri) or vehicle. Toward this end, we orthotopically implanted KI PDAC tumor cells into syngeneic mice. This cell line produces high levels of CSF1 but does not express CSF1R (11). Starting on day 14 postimplantation, we treated mice with either vehicle or the CSF1R tyrosine kinase inhibitor, PLX3397. Additional details on PLX3397 can be found in the Materials and Methods section and published elsewhere (16, 17, 18, 21). Eight days of CSF1Ri treatment resulted in a significant reduction in the number of tumor-infiltrating $CD11b^{+}Ly6G^{-}Ly6C^{Lo}F4/80^{Hi}MHCII^{+}$ macrophages and $CD11b^{+}Ly6G^{-}Ly6C^{Hi}$ monocytes/Mo-MDSCs, but not $CD11b^{+}Ly6G^{+}Ly6C^{+}MHCII^{Low}$ G-MDSCs (Fig. 2A and Supplementary Fig. S1). Microarray analyses of whole-tumor tissue mRNA expression revealed 204 downregulated and 158 upregulated genes following CSF1Ri treatment (Fig. 2B and Supplementary Table S1). As expected, expression of genes indicative of macrophage infiltration, including *Cd68*, *Mrc1*, *Msr1*, and *Csf1r*, was decreased in CSF1Ri-treated tumors (Fig. 2D). The list of downregulated genes was enriched for molecules involved in "inflammatory responses, chemotaxis, myeloid leukocyte-mediated immunity, and proteolysis," consistent with the decreased number of infiltrating macrophages (Fig. 2C and D). The list of upregulated genes was enriched for molecules involved in "antigen presentation, allograft rejection, interferon responses, and T_H1 immunity" (Fig. 2C). This is consistent with the idea that CSF1R blockade can overcome immune suppression. Corresponding to these altered pathways, genes indicative of CTL responses (*Ifng*, *Cd3e*, *Cd8a*, and *Prf1*), T-cell recruitment (*Cxcl10*, *Ccl3*, and *Ccl4*), and IFN responses (e.g., *Ifng*, *Stat1*, *Irf1*, and *Irf9*) were upregulated (Fig. 2E). Array results were also validated by qRT-PCR on a second set of samples (Fig. 2F). To determine the impact of these alterations, we applied these gene lists to existing gene expression datasets from patients with PDAC (22) and found that the core elements of the downregulated gene list were indicative of poor clinical outcomes (Fig. 2G). Taken together, these results suggest that: (1) inhibition of CSF1R signaling in the stromal compartment decreases myeloid responses and reprograms the tumor microenvironment to support T-cell–mediated antitumor immunity and (2) these changes could improve patient outcomes.

CSF1/CSF1R signal blockade selectively kills $CD206^{Hi}$ TAMs

To determine how inhibition of CSF1/CSF1R signaling impacts myeloid responses, we treated tumor-bearing mice with CSF1 neutralizing antibodies for 6, 12, 24, or 48 hours or 8 days and analyzed tumor-infiltrating myeloid cell composition and cell death at these time points. Within the first 6 hours of αCSF1 treatment, total TAM numbers began to decrease. By 8 days, TAM numbers had decreased by approximately 60% (Fig. 3B). TAMs are a heterogeneous population of

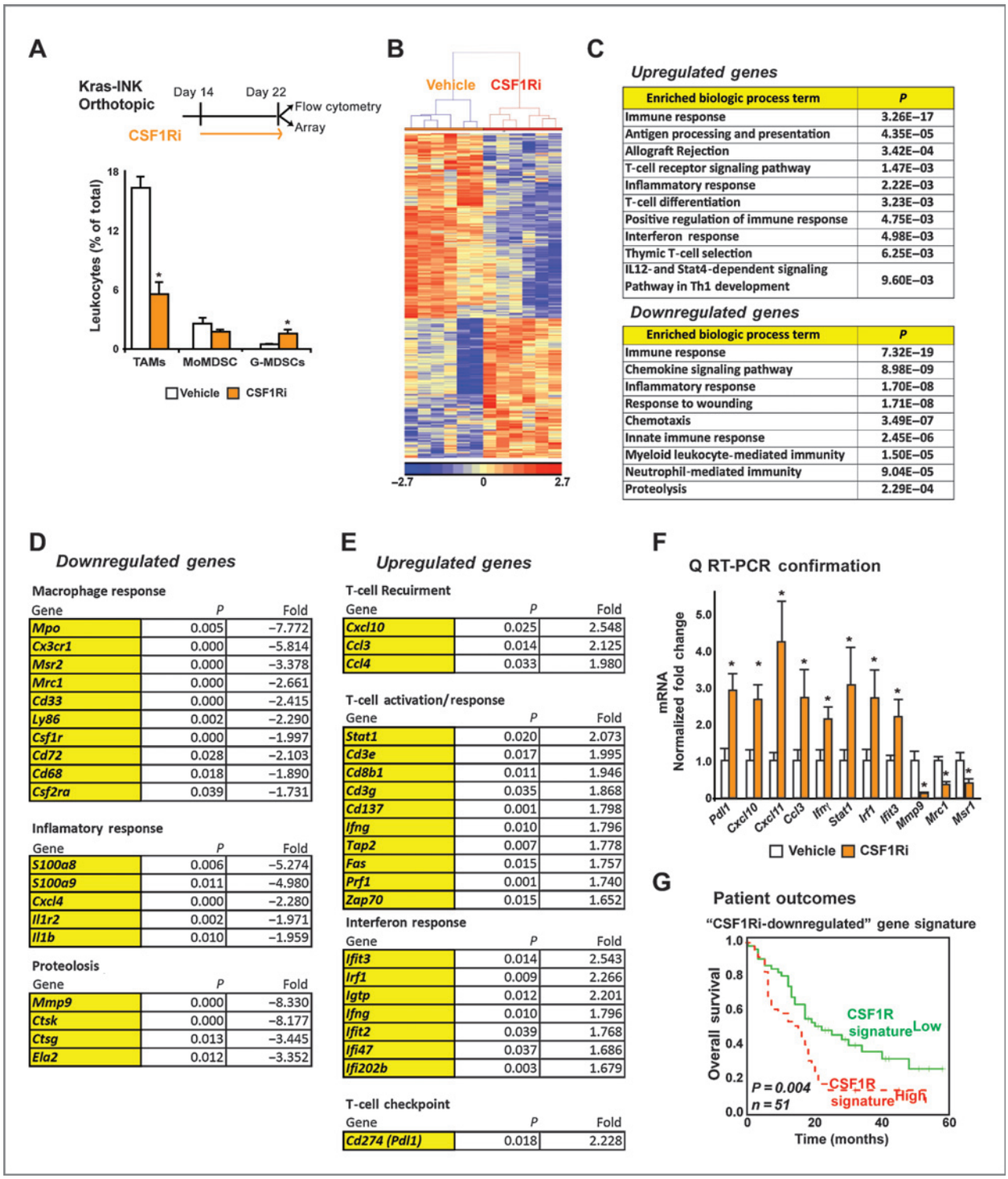

Figure 2. CSF1/CSF1R blockade reprograms the tumor immune microenvironment. A, leukocyte infiltration in KI tumors from mice treated with vehicle or CSF1Ri (PLX3397) for 8 days. The frequency of $CD11b^{+}CD3/19^{-}Ly6G^{-}Ly6C^{Lo}F4/80^{Hi}MHCII^{+}$ macrophages, $CD11b^{+}Ly6G^{-}Ly6C^{Hi}$ Mo-MDSC, and $CD11b^{+}Ly6G^{Hi}Ly6C^{+}MHCII^{low/-}$ G-MDSC subsets is depicted as the mean percentage over total live cells. B, cluster analysis of differential gene expression (Supplementary Table S1) in vehicle- and CSF1Ri-treated tumors. C, table of biologic processes enriched in "upregulated" or "downregulated" genes (DAVID analysis). D–E, selected gene sets are displayed with associated biologic activities. F, qRT-PCR analysis of orthotopic KI tumor tissue following treatment with vehicle or CSF1Ri for 8 days. Graph depicts mean fold-change compared with vehicle. G, Kaplan–Meier analysis of patient cohorts stratified by expression level of genes downregulated from the analysis in B. In all panels $n = 4$–6 mice per group; *, $P < 0.05$ (Mann–Whitney U test), unless specified.

macrophages with diverse biologic activities (23–27). Although classical activation of macrophages can restrain cancer development, alternative activation often plays a protumorigenic role (28, 29). Distinct surface markers have been used to distinguish between classically and alternatively activated macrophages. Murine PDAC tumors contain a distinct subset of $CD206^{Hi}$ TAMs (Fig. 3A and Supplementary Fig. S1), and their counterparts in human pancreatic cancer have been associated with poor clinical outcomes (7). Quantification of $CD206^{Hi}$ and $CD206^{Low}$ TAM subsets revealed that αCSF1 treatment for 8 days led to a >90% depletion of $CD206^{Hi}$ TAMs, whereas $CD206^{Low}$ TAMs decreased by only approximately 45% (Fig. 3C and D). Similar results were seen following CSF1Ri treatment (Fig. 3G). The loss of $CD206^{Hi}$ TAMs could result from either preferential killing of this TAM subset or altered CD206 expression. To distinguish between these possibilities, we analyzed the kinetics of macrophage cell death. We found that in PDAC tumors, $CD206^{Hi}$ TAMs experienced significantly higher levels of cell death following αCSF1 treatment than $CD206^{Low}$ TAMs (Fig. 3D and E). These data suggest that $CD206^{Hi}$ TAMs are more sensitive to the CSF1R signal blockade. Consistent with this differential sensitivity, we found that $CD206^{Hi}$ TAMs express higher levels of CSF1R (Fig. 3F). In addition, although total Mo-MDSCs ($CD11b^{+}$/$Ly6G^{-}$/$Ly6C^{+}$) did not demonstrate decreased infiltration until after 8 days of αCSF1 treatment, $CD206^{Hi}$ Mo-MDSCs were markedly reduced as early as 12 hours after CSF1 neutralization (Supplementary Fig. S2A). In contrast, the number of $CD206^{Low}$ Mo-MDSCs, $CD11b^{+}$/$Ly6G^{+}$/$Ly6C^{-}$/$MHCII^{+}$ mature granulocytes, and $CD11b^{+}$/$Ly6G^{+}$/$Ly6C^{+}$ G-MDSCs remained unaffected until after 8 days of CSF1/CSF1R blockade (Supplementary Fig. S2B). Taken together, these data suggest that the blockade of CSF1/CSF1R signaling preferentially, but not exclusively, depletes $CD206^{Hi}$ TAMs and $CD206^{Hi}$ Mo-MDSCs in pancreatic tumors.

CSF1/CSF1R signaling blockade reprograms TAMs

Despite extensive loss of macrophages and Mo-MDSCs, 40% to 50% of TAMs remain after αCSF1 or CSF1Ri treatment. To determine whether CSF1 blockade reprograms the remaining macrophages to support antitumor activities, we FACS sorted TAMs from 8-day vehicle or αCSF1-treated mice bearing established KI tumors and compared their gene expression profiles. TAMs from αCSF1-treated tumors displayed reduced expression of immunosuppressive molecules, including *Pdcd1lg2*, *Il10*, *Arg1*, *Tgfb1*, and *Ccl22*. In contrast, antitumor immunity genes, such as *Il12a*, *Ifna, Ifnb1, Ifng, Cxcl10*, and *Nos2*, were upregulated (Fig. 3H). We also observed markedly increased surface expression of MHCII after CSF1 or CSF1R inhibition (Fig. 3I). Taken together, these data suggest that the CSF1/CSF1R blockade reprograms remaining TAMs to support antitumor IFN responses and T-cell activities.

CSF1/CSF1R signal blockade alters the function of TAMs and dendritic cells

On the basis of the observed differences in cytokine profiles among TAMs, we predicted that CSF1/CSF1R blockade might also alter the ability of macrophages to suppress T-cell functions. To address this hypothesis, we assessed the immunosuppressive activity and antigen presentation capacity of macrophages in PDAC tumors from mice following CSF1 blockade. Consistent with the reduced expression of immunosuppressive factors (Fig. 3H), we found that FACS-sorted TAMs from 8-day αCSF1-treated mice had significantly reduced ability to block $CD8^{+}$ T-cell activation in *ex vivo* assays (Fig. 4A). These data suggest that the TAMs that remain after CSF1 blockade have reduced immunosuppressive activity.

We also analyzed how CSF1 blockade might impact the number and function of antigen-presenting cells (APC) in the tumor microenvironment. To identify potential APCs in PDAC tumors, we orthotopically implanted mCherry-labeled KI tumor cells. This model allowed us to identify potential APCs by their uptake of tumor antigens, based on their mCherry fluorescence (Fig. 4B; ref. 30). We were able to detect tumor-derived mCherry signal in granulocytes, monocytes, TAMs, and dendritic cells (DC; Fig. 4B). The highest levels of mCherry uptake were observed in TAMs and a subset of $CD11b^{low/-}$/Ly6G/C^{-}/$CD19^{-}$/$CD11c^{+}$/$MHCII^{+}$ cells, presumably lymphoid-like DCs (LyDC). CSF1/CSF1R blockade did not affect mCherry uptake. Interestingly, unlike in TAMs, CSF1/CSF1R blockade significantly increased the number of tumor-infiltrating LyDCs and their surface expression of MHCII (Fig. 4C and Supplementary Fig. S2C–S2E). Because of the high level of tumor antigen uptake by TAMs and LyDCs, we tested the ability of these two cell types to present antigen to naïve $CD8^{+}$ T cells and stimulate their proliferation. We isolated TAMs and LyDCs from orthotopic KC tumors obtained from mice treated with either vehicle or αCSF1 for 8 days. These leukocytes were then loaded with SIINFEKL peptide and assessed for their ability to activate OT1 T cells. Although macrophages and LyDCs isolated from vehicle-treated tumors had very limited ability to activate T cells, αCSF1 treatment significantly enhanced the capacity of these two cell types to induce $CD8^{+}$ T-cell proliferation (Fig. 4D). Taken together, these data suggest that CSF1 blockade alleviates immunosuppressive activities and enhances APC potential in both TAMs and tumor-infiltrating LyDCs.

CSF1/CSF1R blockade modestly increases antitumor T-cell activity

To further understand how the blockade of CSF1/CSF1R signaling might reprogram the tumor microenvironment to regulate tumor progression, we assessed alterations in tumor-infiltrating T lymphocytes and tumor growth following CSF1 or CSF1R blockade in established murine PDAC tumors. Mice bearing established (12 days, ∼1 cm) orthotropic KI or PAN02 tumors were treated with αCSF1 IgGs or CSF1Ri. Tumor progression was modestly reduced by αCSF1 or CSF1Ri treatment as a single agent (Fig. 5A–C). This reduction in tumor growth correlated with increases in $CD3^{+}CD8^{+}$ CTLs and $CD3^{+}CD4^{+}$ effectors T cells, decreases in $CD4^{+}$ $Foxp3^{+}$ T regulatory cells (T_{Reg}s), and significantly improved effector-to-T_{Reg} ratios (Fig. 5D–E). Although the majority of tumor-infiltrating $CD8^{+}$ CTLs had a $CD69^{+}$, $CD44^{+}$, and $CD62L^{-}$ activated phenotype, CSF1R blockade led to a modest increase in both the number of $CD69^{+}$ $CD8^{+}$ T cells (65%–76%) and the

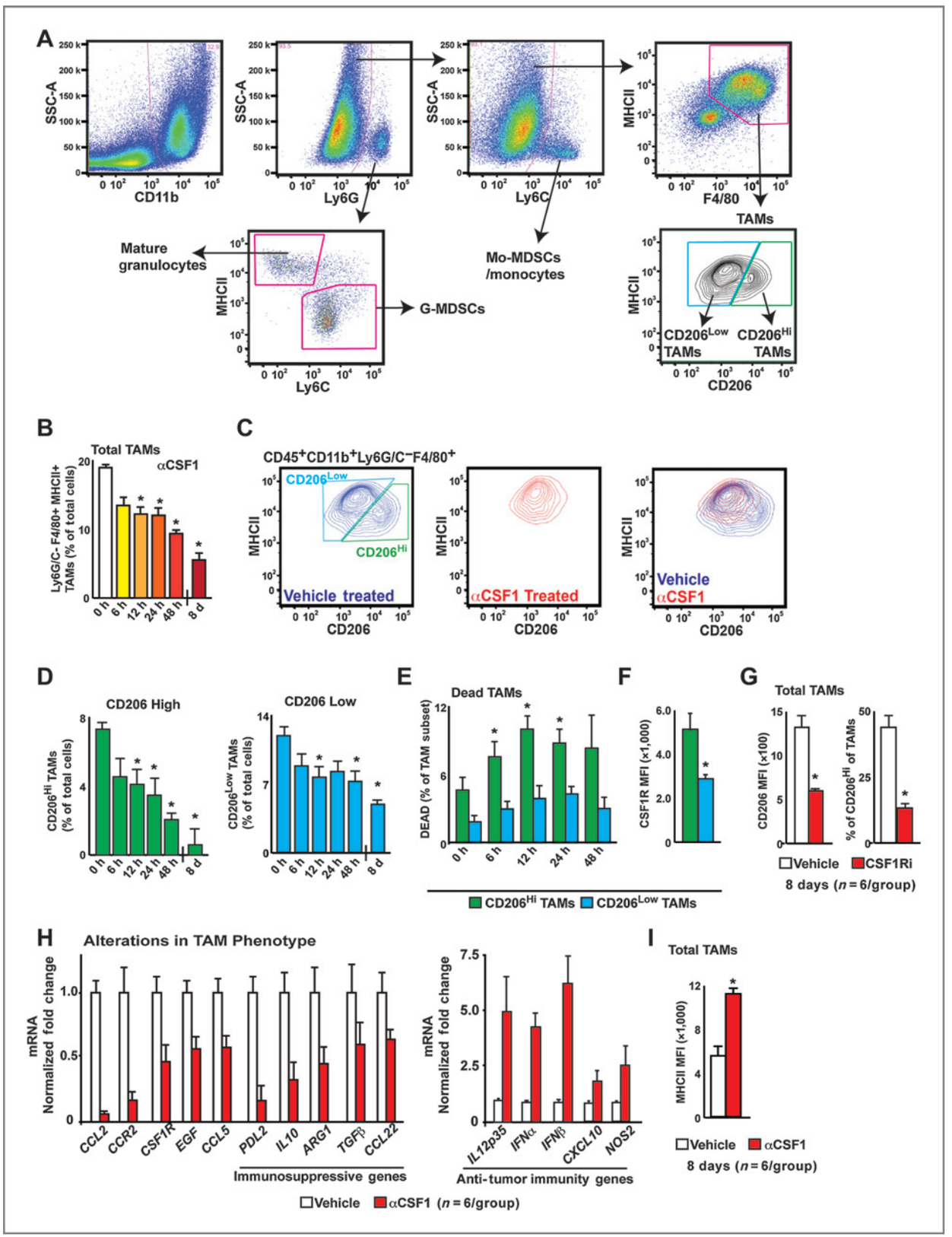
A
SSC-A
CD11b
Ly6G
Ly6C
MHCII
F4/80
Mature granulocytes
G-MDSCs
Mo-MDSCs /monocytes
TAMs
CD206Low TAMs
CD206Hi TAMs
CD206
B
Total TAMs
αCSF1
Ly6G/C- F4/80+ MHCII+ TAMs (% of total cells)
0 h
6 h
12 h
24 h
48 h
8 d
C
CD45+CD11b+Ly6G/C−F4/80+
CD206Low
CD206Hi
Vehicle treated
αCSF1 Treated
Vehicle
αCSF1
D
CD206 High
CD206Hi TAMs (% of total cells)
CD206 Low
CD206Low TAMs (% of total cells)
E
Dead TAMs
DEAD (% of TAM subset)
F
CSF1R MFI (×1,000)
G
Total TAMs
CD206 MFI (×100)
% of CD206Hi of TAMs
Vehicle
CSF1Ri
8 days (n = 6/group)
CD206Hi TAMs
CD206Low TAMs
H
Alterations in TAM Phenotype
mRNA Normalized fold change
CCL2
CCR2
CSF1R
EGF
CCL5
PDL2
IL10
ARG1
TGFβ
CCL22
Immunosuppressive genes
IL12p35
IFNα
IFNβ
CXCL10
NOS2
Anti-tumor immunity genes
Vehicle
αCSF1 (n = 6/group)
I
Total TAMs
MHCII MFI (×1,000)
Vehicle
αCSF1
8 days (n = 6/group)

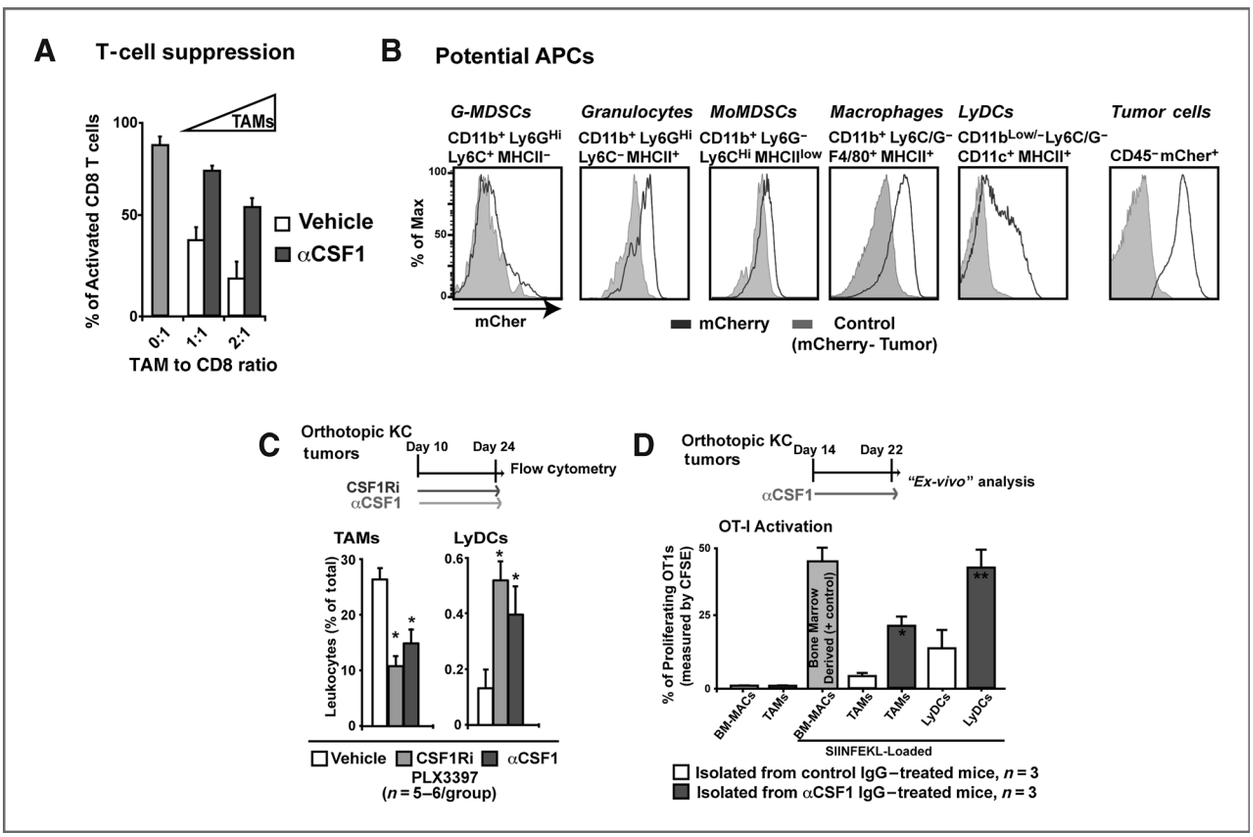

Figure 4. CSF1/CSF1R signaling blockade enhances TAM support for CTL responses. A, analysis of T-cell suppression by TAMs from vehicle- or αCSF1-treated mice. TAMs were isolated by FACS and assayed for their ability to suppress splenic $CD8^+$ T-cell proliferation following anti-CD3/CD28 stimulation. The mean number of proliferation cycles is depicted after 70 hours. Representative data from two replicate experiments ($n = 3$ mice/group). B, flow-cytometric analysis of tumor-derived mCherry fluorescence in tumor-infiltrating leukocytes. Representative plots from five mice are depicted. C, frequency of $CD11b^+$/$Ly6G^-$/$Ly6C^{Lo}$/$F4/80^{Hi}$/$MHCII^+$ TAMs and $CD11b^{Low/-}$/$Ly6GC^-$/$CD19^-$/$CD11c^+$/$MHCII^+$ lymphoid DCs in orthotopic KI tumors after 8 days of αCSF1 or CSF1Ri treatment. D, TAMs and LyDCs were isolated by FACS from mice in C, loaded with SIINFEKL peptide, cocultured with splenic OT1 cells for 18 hours. OT1 proliferation was measured by CFSE dilution. Results reflect two triplicate experiments using three mice per group. All graphs depict mean values ± SEM. *, $P < 0.05$ by an unpaired t test.

level of CD44 expression (Fig. 5F). The observed increase in T-cell numbers and enhancement of activation status correspond to our results from gene expression profiling in Fig. 2.

CSF1/CSF1R signal blockade alters T-cell checkpoint signaling

Although the CSF1/CSF1R blockade enhanced T-cell infiltration, we hypothesized that antitumor immunity might be limited via the engagement of T-cell checkpoints. We found that approximately 70% of activated CTLs had a high level of PD1 expression, which was unaffected by CSF1R blockade. In contrast, CTLA4 expression on $CD8^+$ CTLs was significantly upregulated by CSF1R inhibition (Fig. 5F). Along these lines, our array analysis (Fig. 2) showed that *Cd274* (PDL1) was significantly upregulated following CSF1R blockade. We verified these results using qRT-PCR, and found that both *Cd274* and *Ctla4*, but not *Pdcd1lg2* (PDL2), are upregulated in tumor tissues following CSF1 or CSF1R blockade (Fig. 6A and B). These data suggest that although CSF1 blockade reprograms the tumor microenvironment to enhance effector T cell infiltration, engagement of T cell checkpoints is also enhanced.

To determine the cellular sources of these molecules, we analyzed PDL1, PDL2, and PD1 expression on tumor cells and tumor-infiltrating myeloid cells from vehicle- or CSF1Ri-

Figure 3. CSF1/CSF1R signaling blockade reprograms TAM response. A, representative flow-cytometric plots with gating strategy to identify mature granulocytes, G-MDSCs, Mo-MDSCs, and TAM subsets. B–D, frequency of total $CD206^{Hi}$ and $CD206^{Low}$ TAMs in orthotopic KI tumors treated with αCSF1 for 6 hours to 8 days. Mean percentage of macrophages over total cells is depicted. C, representative analysis of MHCII and CD206 expression in TAMs following 8-day treatment with vehicle or αCSF1. E, analysis of dead (live/dead blue dye^+) $CD206^{Hi}$ and $CD206^{Low}$ TAMs in PDAC tumors from B. F, CSF1R expression by MFI in $CD206^{HI}$ and $CD206^{Low}$ TAMs in vehicle-treated mice from B. G, CD206 expression by MFI and $CD206^{Hi}$ TAM number following 8 days of αCSF1 treatment. H, qRT-PCR analysis on $CD11b^+Ly6G/C^-F4/80^+MHCII^+$ TAMs sorted from KI tumors following 8-day treatment with vehicle or αCSF1. I, MHCII expression by MFI in TAMs from H. All graphs depict means values or normalized fold-change ± SEM, $n = 4$–6 mice per group; *, $P < 0.05$ by an unpaired t test or the Mann–Whitney U test.

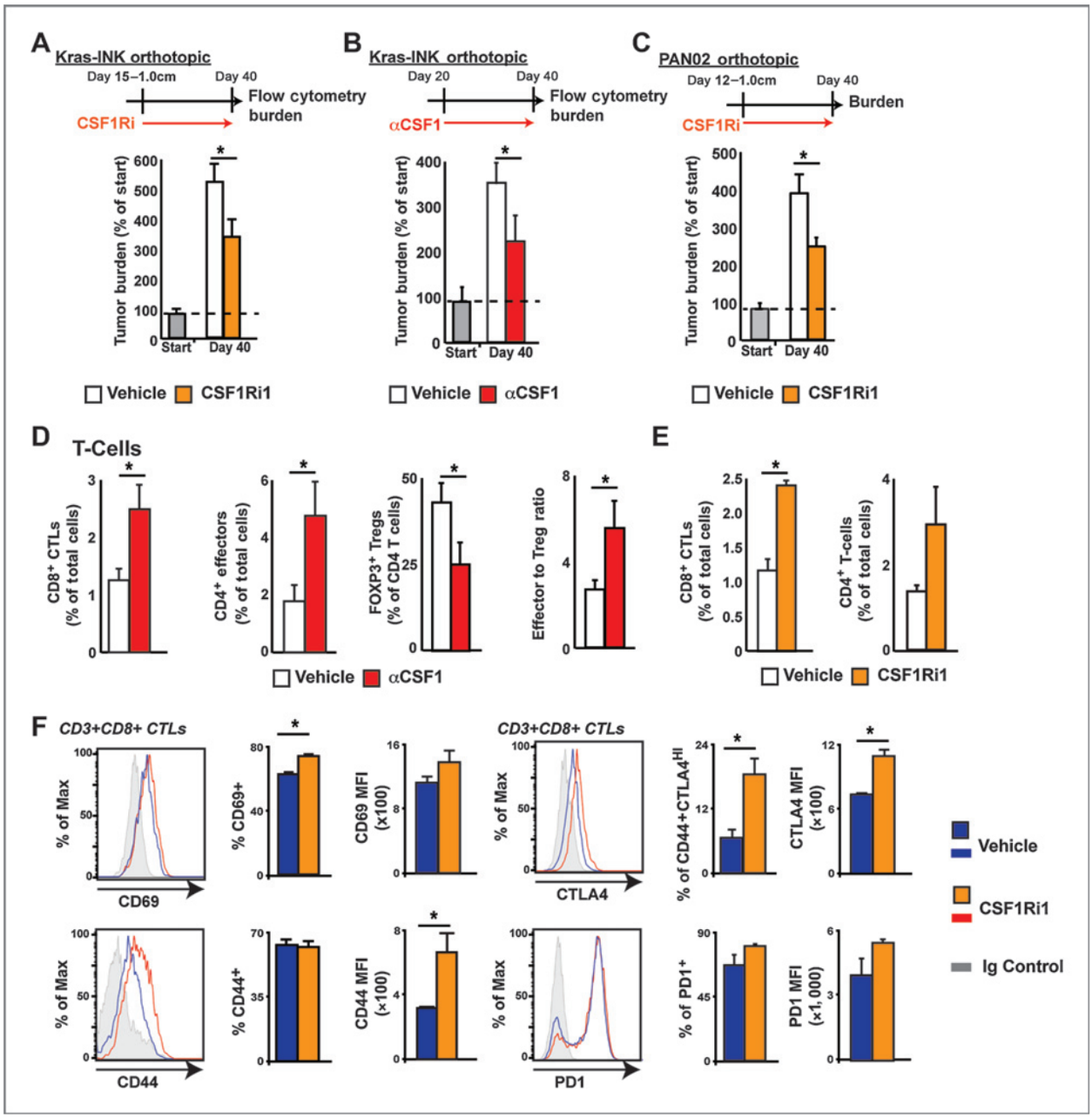

Figure 5. CSF1/CSF1R blockade bolsters T-cell responses. A–C, mice bearing established orthotopic KI or PAN02 tumors were treated with vehicle, CSF1Ri, or αCSF1. Tumor burden is displayed as mean tumor weight ($n = 10$–15 mice/group), normalized to five mice sacrificed at the start of treatment (Start). D–E, analysis of tumor-infiltrating $CD3^+CD8^+$CTLs, $CD3^+CD4^+Foxp3^-$ effector T cells, and $CD4^+Foxp3^+$ T_{reg} from mice in A–B is depicted as mean percentage over total live cells ($n = 6$ mice/group). The mean effector (CTL + $CD4^+$ effector)-to-T_{Reg} ratio is also depicted. F, CD69, CD44, CTLA4, and PD1 expression in $CD3^+CD8^+$CTLs from mice in A is depicted as both MFI and percentage of positive cells. Representative plots are depicted. *, $P < 0.05$ by the Mann–Whitney and $n = 5$–6 in all panels.

treated mice. We found that TAMs expressed high levels of PD1, PDL1, and PDL2, but consistent with a decreased immunosuppressive capacity, tumor-infiltrating macrophages from CSF1Ri-treated mice had markedly decreased PDL2 and PD1 expression (Fig. 6C and 6F). CSF1Ri treatment also decreased the total number of PD1- and PDL2-positive TAMs (Fig. 6D and F). Similar effects were also seen with αCSF1 treatment (data not shown). Neither Mo-MDSCs nor G-MDSCs expressed significant levels of PDL2. Although CSF1R blockade did not alter PD1 or PDL1 expression in G-MDSCs, PDL1 expression was modestly elevated in Mo-MDSCs following CSF1Ri treatment.

Expression of PDL1, PD1, and PDL2 has been reported on human PDAC tumor cells, potentially allowing them to evade immune surveillance by suppressing T-cell function. To

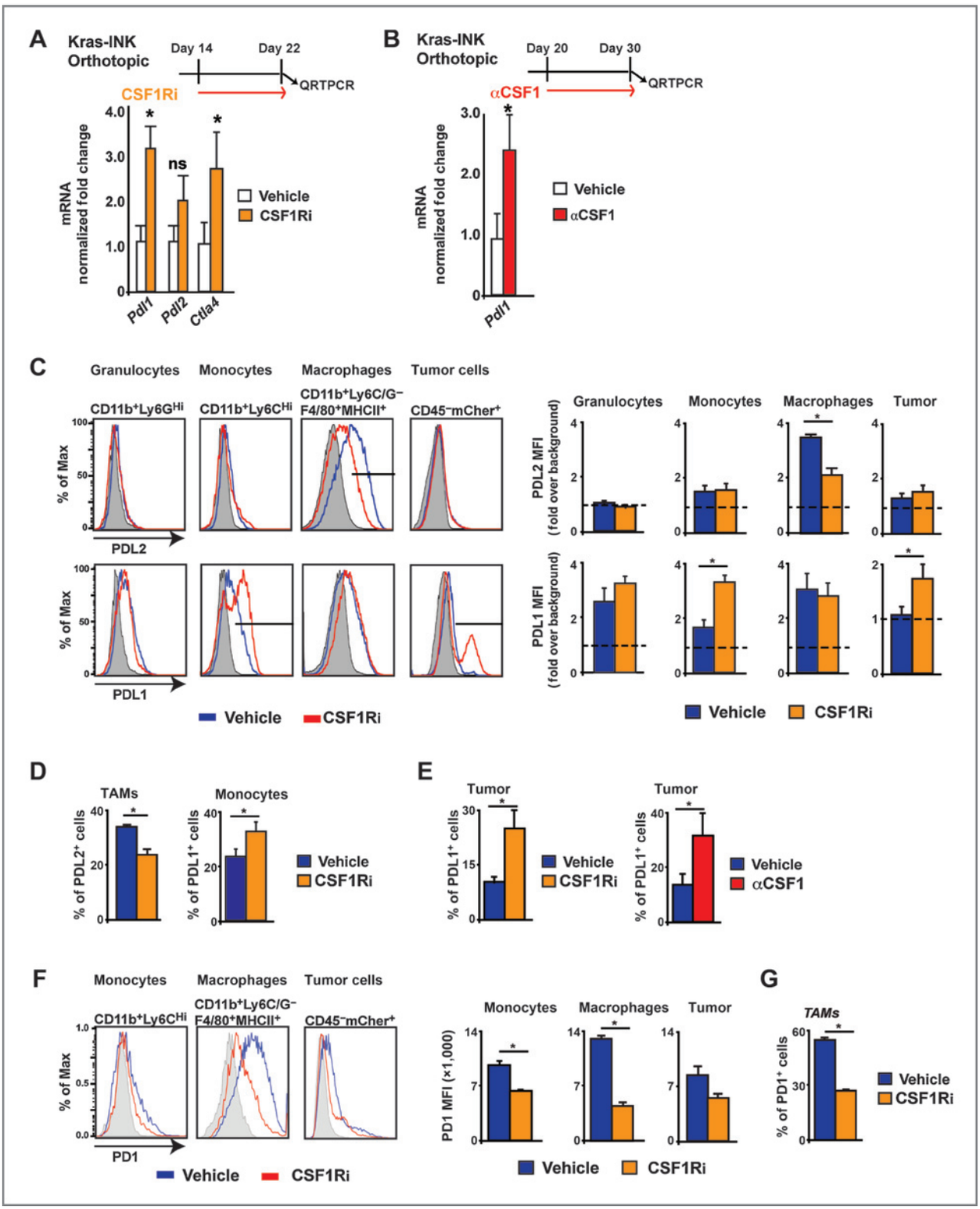

Figure 6. CSF1/CSF1R signaling blockade elevates PDL1 expression in tumor cells. A–B, qRT-PCR analysis of KI tumors following 8-day treatment with vehicle, CSF1Ri, or αCSF1. C, PDL1 and PDL2 expression in denoted tumor-infiltrating myeloid cells from orthotopic KI tumors treated with vehicle or CSF1Ri. Representative FACS plots and MFI are depicted. D, mean percentage of PDL1$^+$ and PDL2$^+$ TAMs and monocytes. E, mean percentage of PDL1$^+$ PDAC cells in orthotopic KI tumors from mice treated with vehicle, CSF1Ri, or αCSF1. PDAC cells were identified as CD45$^-$ mCherry$^+$. F–G, PD1 expression in tumor-infiltrating myeloid cells following vehicle or CSF1Ri treatment. Representative expression plots, MFI, and positive cells percentage data are depicted. All graphs depict mean values ± SEM; $n = 3$–7 mice per group. *, $P < 0.05$ by an unpaired t test.

determine whether CSF1R blockade affects the expression of these molecules on PDAC cells, we used mCherry-expressing KI or KC cells to identify tumor cells *in vivo*. We found that both KI and KC cells express PDL1 at modest levels *in vivo*, but neither cell line expresses PDL2 or PD1 (Fig. 6C and 6F, and not shown). However, following CSF1 or CSF1R blockade, the number of PDL1$^+$ tumor cells and overall expression level of PDL1 were markedly upregulated on PDAC tumor cells (Fig. 6C and 6E). These observations correspond with the increased mRNA levels of *Cd274* identified by array analysis and qRT-PCR validation (Fig. 2 and 6A). Taken together, these results suggest that although CSF1/CSF1R blockade reprograms macrophage responses to bolster CTL responses, this reprogramming also leads to upregulation of PDL1 on tumor cells and CTLA4 on T cells. These checkpoints will likely limit the efficacy of observed antitumor immune responses.

CSF1R blockade enhances responses to checkpoint immunotherapy

On the basis of the above data, we hypothesized that CSF1 or CSF1R blockade could enhance PDAC responses to PD1- and/or CTLA4-antagonist–based immunotherapy. To assess this hypothesis, we treated mice bearing established KI tumors with αPD1 or αCTLA4 with or without CSF1Ri in combination with gemcitabine. PD1 and CTLA4 antagonists in combination with gemcitabine had only limited efficacy at blunting the progression of established tumors (Fig. 7A and B). In contrast, the combination of CSF1R blockade with either PD1 or CTLA4 antagonists reduced tumor progression by more than 90%. Because combined PD1 and CTLA4 antagonist therapy is being tested clinically for the treatment of both melanoma and PDAC, we also tried this combined therapeutic approach. In the absence of chemotherapy, even combined αPD1/αCTLA4 treatment only limited tumor progression by approximately 50%. However, the addition of CSF1R blockade to αPD1/αCTLA4 treatment completely blocked tumor progression and even regressed established tumors by 15% (Fig. 7C). When CSF1 blockade was combined with αPD1/αCTLA4 and gemcitabine treatment, we observed complete tumor regression in 30% of animals and an average tumor regression of approximately 85% (Fig. 7D). Similar results were seen in orthotopic KC tumors, and when the less potent CSF1R inhibitor, GW2850,

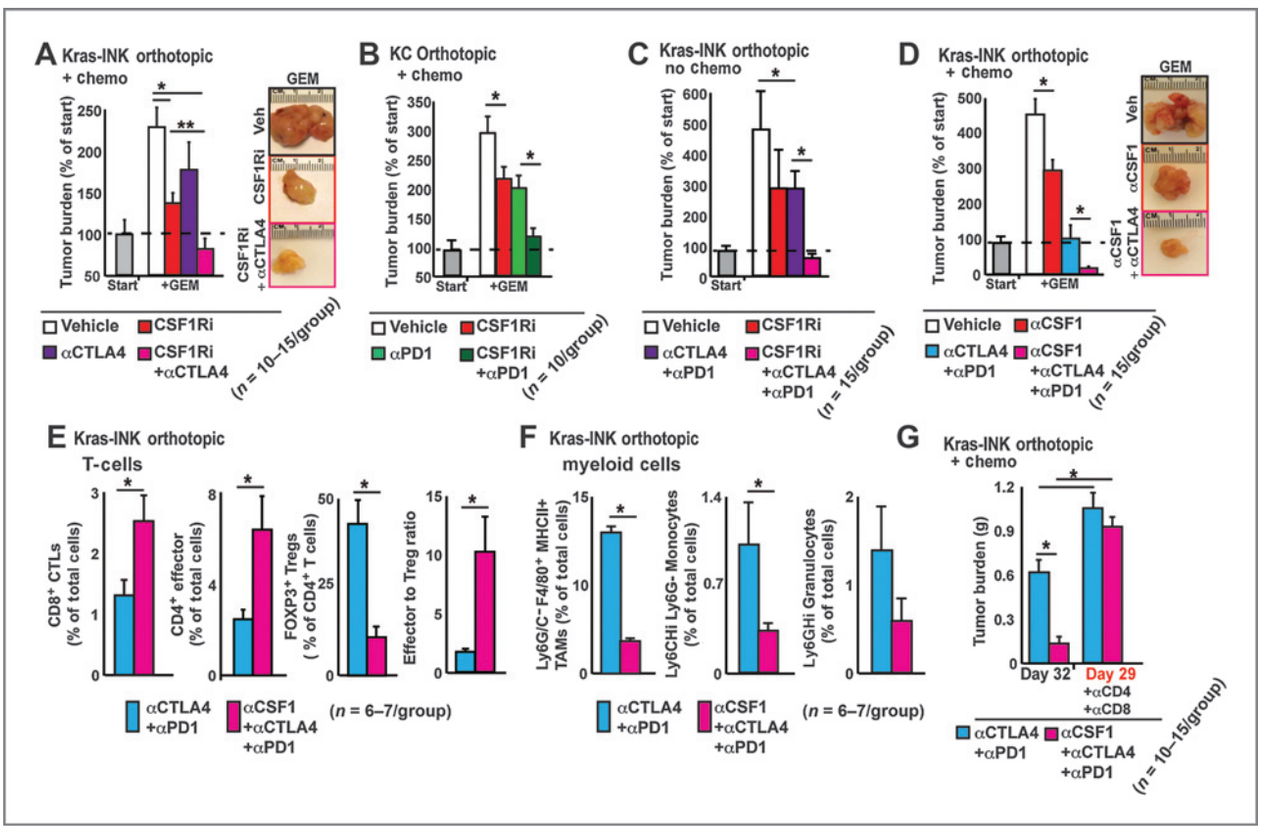

Figure 7. CSF1/CSF1R signaling blockade enhances T-cell checkpoint immunotherapy. A–D, mice bearing orthotopic KI or KC tumors were treated with vehicle, CSF1Ri, or αCSF1, ± gemcitabine ± αPD1, and ±αCTLA4. The tumor burden is displayed as mean tumor weight (n = 10–15 mice/group), normalized to five mice sacrificed at the start of treatment (Start). E, frequency of tumor-infiltrating CD3$^+$CD8$^+$CTLs, CD3$^+$CD4$^+$Foxp3$^-$ T effectors, and Foxp3$^+$ CD4$^+$ T_{Reg}s from mice in D is depicted as mean percentage of total live cells (n = 6 mice/group). Mean effector (CTL + CD4$^+$ effector) to T_{Reg} ratio is depicted. F, flow-cytometric analysis of tumor-infiltrating CD11b$^+$Ly6C/G$^-$F4/80$^+$MHCII$^+$ TAMs, CD11b$^+$Ly6C$^+$Ly6G$^-$ Mo-MDSCs, and CD11b$^+$ Ly6C$^+$ Ly6G$^+$MHCII$^-$ G-MDSCs from mice in D is depicted as mean percentage of total cells (n = 6 mice/group). G, mice bearing orthotopic KI tumors were treated with GEM, αPD1, αCTLA4, vehicle or αCSF1, ± αCD4 and αCD8. The tumor burden is displayed as mean tumor weight (n = 10–15 mice/group). All graphs depict mean values ± SEM; *, $P < 0.05$ by an unpaired t test and/or the Mann–Whitney U test.

was used (Fig. 7B and Supplementary Fig. S3A and S3B). Analysis of T-cell responses following combined therapy with αCSF1 and αPD1/αCTLA4 antagonists demonstrated increased $CD8^+$ CTL and $CD4^+$ effector T-cell infiltration and decreased $CD4^+$ $Foxp3^+$ T_{Reg} numbers (Fig. 7E). In addition, the number of TAMs, Mo-MDSCs, and G-MDSCs decreased following this combined therapeutic regimen (Fig. 7F).

To determine whether alterations in tumor burden in CSF1Ri treatment mice were due to increased T-cell responses, we conducted CD4 and CD8 T depletion studies and found that CSF1R blockade no longer improved checkpoint-based therapy (Fig. 7G). Taken together, these results suggest that CSF1/CSF1R blockade improve checkpoint immunotherapy by enhancing $CD4^+$ and $CD8^+$ T-cell activities.

Discussion

In this report, we show that blockade of CSF1/CSF1R signaling in pancreatic tumors depletes $CD206^{Hi}$ TAMs and reprograms remaining macrophages to support antitumor immunity. The blockade alone modestly enhances antitumor IFN responses, promotes CTL infiltration, and slows tumor progression. However, the therapeutic effect is limited by the induction of T-cell checkpoint molecules, including PDL1 on tumor cells and CTLA4 on T cells. Addition of the CSF1/CSF1R blockade markedly improved the efficacy of αPD1 and αCTLA4 checkpoint immunotherapy and led to the regression of even well-established PDAC tumors. These data suggest that CSF1/CSF1R signaling may be an effective therapeutic target to reprogram the immunosuppressive microenvironment of human PDAC tumors and enhance the efficacy of immunotherapy.

Recent data from several groups suggest that inhibition of CSF1R signaling alters the immunologic responses of tumor-infiltrating macrophages in several cancer types (10–12, 31–33). Mok and colleagues targeted CSF1R signaling using the compound PLX3397 in a murine melanoma model; PLX3397 treatment depleted >80% of TAMs, leaving behind a small population of $MHCII^{Hi}$ macrophages (10). These effects led to increased efficacy of adoptively transferred T-cell–based therapies. These data agree with our report here. In addition, recent work by Pyonteck and colleagues has shown that blockade of CSF1R signaling, using the small-molecule inhibitor BLZ945, significantly blunts murine glioma tumor growth by reprogramming macrophage responses (31). In contrast with pancreas, melanoma, and breast models, macrophage numbers in these murine glioma studies were not reduced. Instead, TAM survival was sustained by tumor-derived factors. However, in glioma, CSF1R blockade impairs the tumor-promoting functions of TAMs and regresses established tumors. Taken together, these results suggest that CSF1/CSF1R signaling can regulate both the number and the function of TAMs, but these activities may be highly dependent on tumor-type/tissue-specific factors.

One possible mechanism by which CSF1Ri reprograms the remaining TAMs is that CSF1R signaling may promote tumor-promoting macrophage phenotypes, while its blockade polarizes TAMs into the antitumor phenotype. In a study by Fleetwood and colleagues, macrophages cultured in CSF1 or CSF2 demonstrated different cytokine profiles and transcription activity (34). For example, in response to lipopolysaccharide, CSF2-derived macrophages preferentially produce IL6, IL12, and TNFα, whereas CSF1-derived macrophages produce IL10 and CCL-2, but not IL12. These data suggest that the exact cytokine milieu differentially program macrophages to play diverse roles. Intriguingly PDAC tumors can also produce high levels of CSF2 (35, 36), which could reprogram TAMs toward DC-like phenotypes when unopposed by CSF1R signaling.

Alternative to TAMs being reprogrammed by CSF1Ri, another possible mechanism is that CSF1R signaling blockade selects for a subset of tumor-restraining macrophages that are insensitive to the CSF signal kills-off a subset of TAMs that have a protumor phenotype. In many physiologic and pathologic settings, including cancers, macrophages are composed of heterogeneous subsets of populations with distinct functions (23). These subsets may depend on different factors for their survival, proliferation, and effector functions. Selection pressure due to CSF1 signal blockade may have enriched for subsets of antitumor macrophages in PDAC tissue that are less dependent on CSF1 signaling for their survival. Our analysis of cell death in $CD206^{Hi}MHCII^{Low}$ versus $CD206^{Lo}MHCII^{Hi}$ TAM sensitivity to αCSF1 IgG supports this hypothesis (Fig. 3B). Although both $CD206^{Hi}$ and $CD206^{Low}$ TAM populations had detectable cell death upon CSF1 neutralization, the $CD206^{Hi}$ populations were preferentially depleted. The $CD206^{Hi}$ TAM subset had significantly higher CSF1R expression levels, suggesting that this population may be more dependent on the CSF1 signal. Taken together, the heterogeneity of macrophages within the tumor tissue suggests that subsets of TAMs can be targeted to modulate the tumor microenvironment and enhance tumor elimination.

CD206 is expressed in many subsets of myeloid cells other than macrophages, including immature dendritic cells and monocytes (37). Whether CD206 expression is correlated to differential activation status in these cell types is not known. Interestingly, $Tie2^+$ monocytes almost uniformly express CD206 (38). It remains to be seen whether the loss of $CD206^{Hi}$ tumor-infiltrating monocytes upon αCSF1 treatment (Supplementary Fig. S2A) involves the $Tie2^+$ monocytes and/or affects tumor vasculature.

Although CSF1/CSF1R blockade enhances the antitumor activity of myeloid cells and T-cell responses, its efficacy can be blunted by upregulation of immune checkpoint molecules, especially PDL1. Although tumor intrinsic pathways have been reported to drive PDL1 expression in tumor cells (4), multiple lines of evidence suggest that PDL1 expression by epithelial tumors is an adaptive response to IFN signaling from tumor stroma. Several groups have reported that IFNγ and IFNα directly lead to the upregulation of PDL1 (39–42). Consistent with these studies, *in vitro* treatment with recombinant IFNγ markedly upregulated PDL1 expression in our PDAC cell lines (not shown). Given the elevated expression of IFNs and IFN response genes in CSF1Ri-treated PDAC tumor tissue, we reason that CSF1Ri-mediated IFN production might drive the upregulation of PDL1 in PDAC cells, an inherent limitation of this therapy.

Even though T-cell checkpoint inhibitors alone have achieved impressive clinical benefits in some other cancers, particularly melanoma (43, 44), their application in pancreatic cancer as single agents has had limited efficacy (3). This is potentially due to the immunosuppressive microenvironment of PDAC tissue, which could be alleviated by therapeutic strategies that reprogram dominant myeloid responses to allow for effective checkpoint therapy.

Disclosure of Potential Conflicts of Interest

D.C. Linehan received commercial research support from Washington University/Pfizer Biomedical Collaborative. No potential conflicts of interest were disclosed by other authors.

Authors' Contributions

Conception and design: Y. Zhu, D.C. Linehan, D.G. DeNardo
Development of methodology: Y. Zhu, D.G. DeNardo
Acquisition of data (provided animals, acquired and managed patients, provided facilities, etc.): Y. Zhu, B.L. Knolhoff, M.A. Meyer
Analysis and interpretation of data (e.g., statistical analysis, biostatistics, computational analysis): Y. Zhu, J. Luo, D.C. Linehan, D.G. DeNardo
Writing, review, and/or revision of the manuscript: Y. Zhu, M.A. Meyer, B.L. West, J. Luo, A. Wang-Gillam, S.P. Goedegebuure, D.C. Linehan, D.G. DeNardo
Administrative, technical, or material support (i.e., reporting or organizing data, constructing databases): Y. Zhu, T.M. Nywening, D.G. DeNardo
Study supervision: D.G. DeNardo
Other (provided agents): A. Wang-Gillam

Grant Support

This work was supported by the Genome Technology Access Center, which is partially supported by NCI Cancer Center Support grant #P30 CA91842 and ICTS/CTSA grant #UL1RR024992. D.G. DeNardo acknowledges the generous support from a Lustgarten Innovation Award, an Edward Mallinckrodt Jr. Award, The Cancer Research Foundation, and a Siteman Cancer Center Career Development Award and R01 CA177670-01. D.C. Linehan acknowledges the Siteman Cancer Frontier Fund and NCI R01 CA168863-01. M.A. Meyer acknowledges funding from the Siteman Cancer Center Cancer Biology Pathway. A. Wang-Gillam acknowledges Washington University Clinical and Translational Grant KL2TR000450. T.M. Nywening acknowledges NCI grant T32 CA 009621.

The costs of publication of this article were defrayed in part by the payment of page charges. This article must therefore be hereby marked *advertisement* in accordance with 18 U.S.C. Section 1734 solely to indicate this fact.

Received January 17, 2014; revised May 29, 2014; accepted June 27, 2014; published OnlineFirst July 31, 2014.

References

1. Gunturu KS, Rossi GR, Saif MW. Immunotherapy updates in pancreatic cancer: are we there yet? Ther Adv Med Oncol 2013;5:81–9.
2. Lutz E, Yeo CJ, Lillemoe KD, Biedrzycki B, Kobrin B, Herman J, et al. A lethally irradiated allogeneic granulocyte-macrophage colony stimulating factor-secreting tumor vaccine for pancreatic adenocarcinoma. A Phase II trial of safety, efficacy, and immune activation. Ann Surg 2011;253:328–35.
3. Royal RE, Levy C, Turner K, Mathur A, Hughes M, Kammula US, et al. Phase 2 trial of single agent Ipilimumab (anti-CTLA-4) for locally advanced or metastatic pancreatic adenocarcinoma. J Immunother 2010;33:828–33.
4. Le DT, Lutz E, Uram JN, Sugar EA, Onners B, Solt S, et al. Evaluation of ipilimumab in combination with allogeneic pancreatic tumor cells transfected with a GM-CSF gene in previously treated pancreatic cancer. J Immunother 2013;36:382–9.
5. Coussens LM, Pollard JW. Leukocytes in Mammary Development and Cancer. Cold Spring Harb Perspect Biol 2010;3:a003285.
6. Pollard JW. Trophic macrophages in development and disease. Nat Rev Immunol 2009;9:259–70.
7. Ino Y, Yamazaki-Itoh R, Shimada K, Iwasaki M, Kosuge T, Kanai Y, et al. Immune cell infiltration as an indicator of the immune microenvironment of pancreatic cancer. Br J Cancer 2013;108:914–23.
8. Balaz P, Friess H, Kondo Y, Zhu Z, Zimmermann A, Buchler MW. Human macrophage metalloelastase worsens the prognosis of pancreatic cancer. Ann Surg 2002;235:519–27.
9. Kurahara H, Shinchi H, Mataki Y, Maemura K, Noma H, Kubo F, et al. Significance of M2-polarized tumor-associated macrophage in pancreatic cancer. J Surg Rese 2011;167:e211–9.
10. Mok S, Koya RC, Tsui C, Xu J, Robert L, Wu L, et al. Inhibition of CSF-1 receptor improves the antitumor efficacy of adoptive cell transfer immunotherapy. Cancer Res 2014;74:153–61.
11. Mitchem JB, Brennan DJ, Knolhoff BL, Belt BA, Zhu Y, Sanford DE, et al. Targeting tumor-infiltrating macrophages decreases tumor-initiating cells, relieves immunosuppression, and improves chemotherapeutic responses. Cancer Res 2013;73:1128–41.
12. DeNardo DG, Brennan DJ, Rexhepaj E, Ruffell B, Shiao SL, Madden SF, et al. Leukocyte complexity predicts breast cancer survival and functionally regulates response to chemotherapy. Cancer Discov 2011;1:54–67.
13. Tsai J, Lee JT, Wang W, Zhang J, Cho H, Mamo S, et al. Discovery of a selective inhibitor of oncogenic B-Raf kinase with potent antimelanoma activity. Proc Natl Acad Sci U S A 2008;105:3041–6.
14. Artis DR, Bremer R, Gillette S, Hurt CR, Ibrahim PL, Zuckerman RLinventors; Plexxikon, Inc., assignee. Molecular Scaffolds for Kinase Ligand Development. United States; 2005.
15. Conway JG, McDonald B, Parham J, Keith B, Rusnak DW, Shaw E, et al. Inhibition of colony-stimulating-factor-1 signaling *in vivo* with the orally bioavailable cFMS kinase inhibitor GW2580. Proc Natl Acad Sci U S A 2005;102:16078–83.
16. Collisson EA, Sadanandam A, Olson P, Gibb WJ, Truitt M, Gu S, et al. Subtypes of pancreatic ductal adenocarcinoma and their differing responses to therapy. Nat Med 2011;17:500–3.
17. Roy LD, Sahraei M, Subramani DB, Besmer D, Nath S, Tinder TL, et al. MUC1 enhances invasiveness of pancreatic cancer cells by inducing epithelial to mesenchymal transition. Oncogene 2011;30:1449–59.
18. Kim MP, Evans DB, Wang H, Abbruzzese JL, Fleming JB, Gallick GE. Generation of orthotopic and heterotopic human pancreatic cancer xenografts in immunodeficient mice. Nat Protoc 2009;4:1670–80.
19. Pyonteck SM, Gadea BB, Wang HW, Gocheva V, Hunter KE, Tang LH, et al. Deficiency of the macrophage growth factor CSF-1 disrupts pancreatic neuroendocrine tumor development. Oncogene 2012;31:1459–67.
20. Jiao X, Sherman BT, Huang da W, Stephens R, Baseler MW, Lane HC, et al. DAVID-WS: a stateful web service to facilitate gene/protein list analysis. Bioinformatics 2012;28:1805–6.
21. Schubert C, Schalk-Hihi C, Struble GT, Ma HC, Petrounia IP, Brandt B, et al. Crystal structure of the tyrosine kinase domain of colony-stimulating factor-1 receptor (cFMS) in complex with two inhibitors. The Journal of biological chemistry. 2007;282:4094–101.
22. Stratford JK, Bentrem DJ, Anderson JM, Fan C, Volmar KA, Marron JS, et al. A six-gene signature predicts survival of patients with localized pancreatic ductal adenocarcinoma. PLoS Med 2010;7:e1000307.
23. Movahedi K, Laoui D, Gysemans C, Baeten M, Stange G, Van den Bossche J, et al. Different tumor microenvironments contain functionally distinct subsets of macrophages derived from Ly6C(high) monocytes. Cancer Res 2010;70:5728–39.
24. Mantovani A, Sica A. Macrophages, innate immunity and cancer: balance, tolerance, and diversity. Curr Opin Immunol 2010;22:231–7.
25. Martinez FO, Sica A, Mantovani A, Locati M. Macrophage activation and polarization. Front Biosci 2008;13:453–61.
26. Mantovani A. From phagocyte diversity and activation to probiotics: back to Metchnikoff. Eur J Immunol 2008;38:3269–73.
27. Qian BZ, Pollard JW. Macrophage diversity enhances tumor progression and metastasis. Cell 2010;141:39–51.
28. Mosser DM, Edwards JP. Exploring the full spectrum of macrophage activation. Nat Rev Immunol 2008;8:958–69.

29. Martinez FO, Helming L, Gordon S. Alternative activation of macrophages: an immunologic functional perspective. Annu Rev Immunol 2009;27:451–83.
30. Engelhardt JJ, Boldajipour B, Beemiller P, Pandurangi P, Sorensen C, Werb Z, et al. Marginating dendritic cells of the tumor microenvironment cross-present tumor antigens and stably engage tumor-specific T cells. Cancer Cell 2012;21:402–17.
31. Pyonteck SM, Akkari L, Schuhmacher AJ, Bowman RL, Sevenich L, Quail DF, et al. CSF-1R inhibition alters macrophage polarization and blocks glioma progression. Nat Med 2013;19:1264–72.
32. Priceman SJ, Sung JL, Shaposhnik Z, Burton JB, Torres-Collado AX, Moughon DL, et al. Targeting distinct tumor-infiltrating myeloid cells by inhibiting CSF-1 receptor: combating tumor evasion of antiangiogenic therapy. Blood 2010;115:1461–71.
33. Strachan DC, Ruffell B, Oei Y, Bissell MJ, Coussens LM, Pryer N, et al. CSF1R inhibition delays cervical and mammary tumor growth in murine models by attenuating the turnover of tumor-associated macrophages and enhancing infiltration by CD8 T cells. Onco Immunol 2013;2:e26968.
34. Fleetwood AJ, Lawrence T, Hamilton JA, Cook AD. Granulocyte-macrophage colony-stimulating factor (CSF) and macrophage CSF-dependent macrophage phenotypes display differences in cytokine profiles and transcription factor activities: implications for CSF blockade in inflammation. J Immunol 2007;178: 5245–52.
35. Pylayeva-Gupta Y, Lee KE, Hajdu CH, Miller G, Bar-Sagi D. Oncogenic Kras-Induced GM-CSF Production Promotes the Development of Pancreatic Neoplasia. Cancer Cell 2012;21:836–47.
36. Bayne LJ, Beatty GL, Jhala N, Clark CE, Rhim AD, Stanger BZ, et al. Tumor-derived granulocyte-macrophage colony-stimulating factor regulates myeloid inflammation and T cell immunity in pancreatic cancer. Cancer Cell 2012;21:822–35.
37. Van Dyken SJ, Locksley RM. Interleukin-4- and interleukin-13-mediated alternatively activated macrophages: roles in homeostasis and disease. Ann Rev of Immunol 2013;31:317–43.
38. Pucci F, Venneri MA, Biziato D, Nonis A, Moi D, Sica A, et al. A distinguishing gene signature shared by tumor-infiltrating Tie2-expressing monocytes, blood "resident" monocytes, and embryonic macrophages suggests common functions and developmental relationships. Blood 2009;114:901–14.
39. Chen J, Feng Y, Lu L, Wang H, Dai L, Li Y, et al. Interferon-gamma-induced PD-L1 surface expression on human oral squamous carcinoma via PKD2 signal pathway. Immuno Biol 2012;217:385–93.
40. Spranger S, Spaapen RM, Zha Y, Williams J, Meng Y, Ha TT, et al. Up-regulation of PD-L1, IDO, and T(regs) in the melanoma tumor microenvironment is driven by CD8(+) T cells. Sci Translational Med 2013;5:200ra116.
41. Terawaki S, Chikuma S, Shibayama S, Hayashi T, Yoshida T, Okazaki T, et al. IFN-alpha directly promotes programmed cell death-1 transcription and limits the duration of T cell-mediated immunity. J Immunol 2011;186:2772–9.
42. Rowe JH, Ertelt JM, Way SS. Innate IFN-gamma is essential for programmed death ligand-1-mediated T cell stimulation following Listeria monocytogenes infection. J Immunol 2012;189:876–84.
43. Hamid O, Robert C, Daud A, Hodi FS, Hwu WJ, Kefford R, et al. Safety and tumor responses with lambrolizumab (anti-PD-1) in melanoma. N Engl J Med 2013;369:134–44.
44. Wolchok JD, Kluger H, Callahan MK, Postow MA, Rizvi NA, Lesokhin AM, et al. Nivolumab plus ipilimumab in advanced melanoma. N Engl J Med 2013;369:122–33.